3. Kim, Y. I.; Park, J. Y.; Choi, S. N. *J. Kor. Chem. Soc.* **1990**, *34*, 108.
4. Choi, S. N.; Park, J. H.; Kim, Y. I.; Shim, Y. B. *Bull. Kor. Chem. Soc.* **1991**, *12*, 276.
5. Choi, S. N.; Kim, Y.; Kim, Y. I. unpublished results.
6. Kim, Y. I.; Choi, S. N.; Kim, J. S.; Kim, H. K. *J. Kor. Chem. Soc.* **1988**, *32*, 122.
7. Brown, D. B.; Crawford, V. H.; Hall, J. W.; Hatfield, W. E. *J. Phy. Chem.* **1977**, *81*, 1303.
8. Wilson, R. B.; Wasson, J. R.; Hatfield, W. E.; Hodgson, D. J. *Inorg. Chem.* **1978**, *17*, 641.
9. Choi, S. N.; Bereman, R. D.; Wasson, J. R. *J. Inorg. Nucl. Chem.* **1975**, *37*, 2087.
10. Wilson, R. B; Wasson, J. R.; Hatfield, W. E.; Hodgson, D. J. *Inorg. Chem.* **1978**, *17*(3), 641.
11. Aoi, Nobuo; Matsubayashi, Gen-etsu; Tanaka, Toshio *J. Chem Soc., Dalton Trans.* **1983**, 1059.
12. Amundsen, A. R.; Whelan, J.; Bosnich, B. *J. Am. Chem. Soc.* **1977**, *99*, 6730.
13. Wasson, J. R.; Richardson, H. W.; Hatfield, W. E. *Z. Naturforsch* **1977**, *326*, 551.
14. (a) Scharnoff, M. *J. Chem. Phys.* **1965**, *42*, 3383; (b) Scharnoff, M.; Reimann, C. W. *J. Chem. Phys.* **1965**, *43*, 2993.
15. Kim, W. S.; Y. I.; Choi, S. N. *Bull. Kor. Chem. Soc.* **1990**, *11*, 85.
16. (a) Tolman, C. A.; Riggs, W. M.; Linn, W. J.; King, C. M.; Wendt, R. C. *Inorg. Chem.* **1973**, *12*, 2770; (b) Colpas, G. J.; Maroney, M. J.; Bagyinka, C.; Kumar, M.; Wills, W. S.; Suib, S. L. *Inorg. Chem.* **1991**, *30*, 920.
17. Wallbank, B.; Main, I. G.; Johnson, C. E. *J. Electron Spectrosc. Relat. Phenom.* **1974**, *5*, 259.
18. Van der Laan, G; Westra, C.; Hass, C.; Sawatzky, G. A. *Phy. Rev.* **1981**, *B23*, 4369.
19. Gewirth, A. A.; Cohen, S. L.; Schugar, H. J.; Solomon, E. I. *Inorg. Chem.* **1987**, *26*, 1133.
20. Srivastava, S. *Apply. Spectro. Rev.* **1986**, *22*, 401.
21. Walton, R. A. *Inorg. Chem.* **1980**, *19*, 1100.
22. Figgis, B. N.; Lewis, J. *The Magnetic Properties of Transition Metal Complexes*; *Prog. Inorg. Chem.* **1964**, *6*, 37, John-Wiely & Son, Inc.: N. Y.
23. Gregson, A. K.; Moxon, N. T.; Weller, R. R.; Hatfield, W. E. *Aust. J. Chem.* **1982**, *35*, 1537.
24. Corvan, P. J.; Estes, W. E.; Weller, R. R.; Hatfield, W. E. *Inorg. Chem.* **1980**, *19*, 1297.

An NMR Study on Molecular Motions of α,2,6-Trichlorotoluene in Solution State

Sangdoo Ahn and Jo Woong Lee*

Department of Chemistry
College of Natural Sciences and Research Institute of Molecular Science
Seoul National University, Seoul 151-742, Korea
Received February 12, 1994

Dynamics of CH_2Cl group in α,2,6-trichlorotoluene dissolved in $CDCl_3$ was studied by observing various relaxation modes for ^{13}C under proton undecoupled condition. Partially relaxed ^{13}C spectra were obtained at 34℃ as a function of evolution time after applying various designed pulse sequences to this AX_2 spin system. It was found that nonlinear regression analysis of the relaxation data for these magnetization modes could provide the information about dipolar and spin-rotational auto-correlation and cross-correlation spectral densities for fluctuation of the ^{13}C-^1H internuclear vector inCH_2Cl group. The results show that the effect of cross-correlation is comparable in magnitude to that of auto-correlation and the relaxation in this spin system is dominated by dipolar mechanism rather than spin-rotational one. From the resulting spectral density data we could calculate the bond angle ∠HCH (105.1°) and elements of the rotational diffusion tensor for CH_2Cl group.

Introduction

The theory describing intramolecular nuclear magnetic relaxation phenomena in multispin systems is nowadays well established and has been shown to be a very powerful tool for the study of dynamics and structure of molecules in liquid.[1-4] For spin 1/2 nuclei, such as ^1H and ^{13}C, in small molecules the most important relaxation mechanisms are known to be the inter- and intramolecular dipole-dipole interactions modulated by molecular reorientation and the spin-rotation interactions modulated by random fluctuation in molecular rotational angular momenta. The dipolar mechanism is usually much more prevailing over the spin-rotational one, but if a system can easily undergo the change in rotational motions, then the contribution from the latter may be substantial.

In a previous investigation[5] we have studied the spin-lattice relaxation of ^{13}C and ^1H spins in methyl group of 2,6-dichlorotoluene dissolved in $CDCl_3$ at 34℃. The result showed that the spin-rotational contribution to the total relaxation rate was found to be about 20%, which indicates that the internal rotation of methyl group is quite fast and facile in

*To whom correspondence should be made.

2,6-dichlorotoluene. However, such may not be the case for internal rotation of a less symmetrical group such as CH_2Cl group in α,2,6-trichlorotoluene. The present paper is concerned with the ^{13}C spin-lattice relaxation in CH_2Cl group of α,2-6-trichlorotoluene, which comprises an AX_2 spin system, and demonstrates that all the information regarding the spectral densities necessary for the study of motional behavior of CH_2Cl group can be obtained through observation of various magnetization modes. This is in contrast to the measurement of T_1, where only one specific mode is observed, thus providing information of only one out of several available spectral densities. The present study also confirms the presence and importance of cross-correlational effect in a coupled spin system which has been regarded as a theoretical curiosity for long time. It is shown that the knowledge of such spectral densities can be utilized to extract the molecular structural and dynamic information.

The study of cross- and auto-correlational effect on spin-lattice relaxation in coupled spin systems has been pioneered by Grant,[1,2,4,6-11] Vold and Vold,[12-15] and others.[16,17] Grant and coworkers have dealt with methylene halide, while Vold and coworkers have worked with simple planar molecules in solution. Compared to these, our system, α,2,6-trichlorotoluene, is a little more complex due to the presence of the internal rotation of CH_2Cl group as well as the anisotropic structure and rotational motion of the molecule as a whole. The techniques described in this paper can be applied to many other molecules (polymers, biomolecules, etc.) involving coupled spin systems as well.

Theory

Underlying theories for the spin relaxation phenomena in liquids have been formulated and advanced by Bloch and by many others.[18-22] Nowadays, Redfield's method of formulation has been quite popular since it is a straightforward matter to extend this formulation to describe the time-dependent nuclear spin dynamics explicitly in terms of the relaxation matrix. In a series of papers Werbelow *et al.*[1,2,6,8] have treated in detail the relaxation in weakly coupled spin systems based on this formalism in terms of spherical tensor operators and symmetry-adapted magnetization modes. Following their treatment we will briefly review the relaxation theory for an AX_2 spin system.

The Hamiltonian of a system of spins and their molecular surroundings can be written in the form

$$\hbar H = \hbar[H_0 + H_1(t)] \tag{1}$$

where H_0 is a large time-independent interaction Hamiltonian (*e.g.* Zeeman interaction, spin-spin coupling, etc.), and $H_1(t)$ is a small time-dependent perturbation (*i.e.* dipolar, spin-rotation, scalar, anisotropic chemical shift interactions, etc.).

The time evolution of the spin density operator, $\chi(t)$, can be described by Liouville-von Neumann equation

$$(d/dt)\chi(t) = -i[H, \chi(t)], \tag{2}$$

which, when carried to second order in $H(t)$, can be more conveniently rewritten in the following form:

$$\frac{d\chi_{aa'}(t)}{dt} = \sum_{b,b'} R_{aa'bb'}[\chi_{bb'}(t) - \chi^T_{bb'}]. \tag{3}$$

The elements of relaxation matrix $\boldsymbol{R}$ can be divided, into two parts originating from dipole-dipole and random field interactions, respectively. That is,

$$R_{aa'bb'} = \sum_{i<j;k<l} R^{ij,kl}_{aa'bb'} + \sum_{i<j} R^{ij}_{aa'bb'}, \tag{4}$$

which can be explicitly expressed in terms of the irreducible spherical tensor operators and the components of spectral densities as shown later.

For dipole-dipole mechanism, the spectral densities take the form

$$J^{mn}_{ijkl}(\omega) = \xi_{ij}\xi_{kl}\int_0^\infty \langle Y^m_2[\Omega_{ij}(0)]Y^n_2[\Omega_{kl}(t)]\rangle \cos(\omega t)dt, \tag{5}$$

where ij and kl represent pairs of interacting spins and ξ_{ij} is the dipolar coupling constant for the ij spin pair separated by the internuclear distance r_{ij}, that is, $\xi_{ij} = (6\pi/5)^{1/2}(\gamma_i\gamma_j\hbar r_{ij}^{-3})$ with γ_i and γ_j denoting magnetogyric ratios of spin i and j, respectively. Also, $\Omega_{ij}(t)$ denotes the orientation of internuclear vector r_{ij} at time t with respect to the laboratory-fixed coordinates.

In the discussion of dipole-diple relaxation in a CH_2 (AX_2) spin system, four dipolar spectral densities, J_{CH}, J_{HH}, J_{CHH}, and J_{HCH}, emerge. These dipolar spectral densities can be expressed as a linear combination of the Fourier transforms of time-dependent correlation functions involving various elements of the second-order Wigner rotation matrix which may be evaluated if a suitable molecular rotational model is found. For example, if the molecular reorientation can be well described by the rotational diffusion model, the method due to Favro[23] can serve for our purpose. One way or the other, we may be able to extract the information regarding the elements of rotational diffusion tensor and the molecular structure parameters from four dipolar spectral densities, J_{CH}, J_{HH}, J_{CHH}, and J_{HCH}.[8]

Random field spectral densities can be expressed as

$$j^{mn}_{ij}(\omega) = \gamma_i\gamma_j\int_0^\infty \langle B^m_1(i,t)B^n_1(j,t)\rangle \cos(\omega t)dt, \tag{6}$$

where $B^m_1(i,t)$ is the lattice component of the magnetic field at the position of nucleus i. These random field terms primarily account for the effect due to paramagnetic impurities, the chemical shift anisotropy (CSA) interactions, and the spin-rotation interactions. Since paramagnetic impurities are usually removed in the process of sample preparation (degassing) and the effect due to CSA interactions is conspicuous only in the presence of high magnetic field, we are left with the spin-rotation interaction only in our case.

Eq. (3) may be rewritten in terms of various normalized magnetization modes v_i's for a given spin system as follows:

$$-\frac{dv_i(t)}{dt} = \sum_j R_{ij}[v_j(t) - v^T_j], \tag{7}$$

where v^T_j means the thermal equilibrium value for the v_j mode.

For AX_2 spin system, Eq.(7) represents a set of eight

Table 1. Magnetization modes and elements of relaxation matrix for AX_2 spin system

E
${}^sv_1 = Tr[I_z^A(I_z^{X_1}+I_z^{X_2})\chi]$
${}^sv_2 = \sqrt{2}Tr[I_z^{X_1}I_z^{X_2}\chi]$
${}^sv_3 = (1/2)Tr[(I_+^{X_1}I_-^{X_2}+I_-^{X_1}I^{X_2})\chi]$
${}^av_1 = Tr[I_z^A\chi]$
${}^av_2 = (1/\sqrt{2})Tr[(I_z^{X_1}+I_z^{X_2})\chi]$
${}^av_3 = 4Tr[I_z^AI_z^{X_1}I_z^{X_2}\chi]$
${}^av_4 = \sqrt{2}Tr[(I_+^{X_1}I_-^{X_2}+I_-^{X_1}I_+^{X_2})I_z^A\chi]$
${}^sR_{11} = (16/3)J_{AX}+5J_{XX}+2J_{XAX}+2j_A+2j_X$
${}^sR_{12} = -(5/3)J_{XAX}-2J_{AXX}$
${}^sR_{13} = 2\sqrt{2}[(5/6)J_{AX}+J_{AXX}]$
${}^sR_{22} = (20/3)J_{AX}+J_{XX}-(10/3)J_{XAX}+4j_X-2j_{XX}$
${}^sR_{23} = -2\sqrt{2}[(1/2)J_{XX}+(5/3)J_{XAX}+j_{XX}]$
${}^sR_{33} = (20/3)J_{AX}+2J_{XX}+4j_X$
${}^aR_{11} = (20/3)J_{AX}+2j_A$
${}^aR_{12} = (5\sqrt{2}/3)J_{AX}$
${}^aR_{13} = 2J_{XAX}$
${}^aR_{14} = (7\sqrt{2}/3)J_{XAX}$
${}^aR_{22} = (10/3)J_{AX}+5J_{XX}+2j_X$
${}^aR_{23} = 2\sqrt{2}J_{AXX}$
${}^aR_{24} = (5/3)J_{XAX}-2J_{AXX}$
${}^aR_{33} = 4J_{AX}+2J_{XX}+2j_A+4j_X$
${}^aR_{34} = -\sqrt{2}(J_{XX}+J_{XAX}+2j_{XX})$
${}^aR_{44} = (14/3)J_{AX}+J_{XX}-(4/3)J_{XAX}+2j_A+4j_X-2j_{XX}$

*We have the adopted abbreviated notations J_{AX}, J_{XX}, J_{AXX}, J_{XAX} instead of J_{AXAX}, $J_{XX'XX'}$, $J_{AXXA'}$, $J_{XAAX'}$, respectively.

coupled simultaneous linear differential equations involving the symmetry-adapted magnetization modes. Four symmetric modes, four antisymmetric modes (distinguished by inversion symmetry), and elements of the relaxation matrix R_{ij} involved in Eq. (7) are listed in Table 1. For computational simplicity, we have used the normalized and symmetric set of magnetization modes originally described by Werbelow and Grant.[8]. The symmetric mode, E, is totally symmetric so that symmetric relaxation matrix is reduced to a 1 by 1 and a 3 by 3 matrix. And we assume the extreme narrowing condition is valid throughout our discussion so that we need not worry about the frequency dependencies of spectral densities involved.

Among eight available magnetization modes the following four are known to be directly observable:

- ${}^sv_1$, the difference between the two outer lines in the carbon triplet,
- ${}^av_1$, the total carbon magnetization,
- ${}^av_2$, the total proton magnetization, and
- ${}^av_3$, the sum of the outer two lines minus the central line of carbon triplet.

In this work we will be concerned with three carbon observable modes only.

Experiment and Results

α,2,6-Trichlorotoluene (97%) and $CDCl_3$(100%) were purchased from Aldrich Chemical Co. and used without further purification. 1.0 M $CDCl_3$ solution of α,2,6-trichlorotoluene was placed in a 10 *mm* o.d. NMR tube and was degassed by repeating the freeze-pump-thaw cycles 6 times and sealed under vacuum. All the relaxation measurements were performed at the temperature of 307 K on a Varian VXR-200S NMR spectrometer operating at ^{13}C resonance frequency of 50.29 MHz. After applying the carbon π pulses with or without application of selective and nonselective proton π pulses the relaxation behaviors of various magnetization modes were observed with the proton couplings allowed. The length of a ^{13}C 180° pulse used was 33 μsec. Pulse delay was taken to be longer than $10T_1$ to ensure that the magnetization be completely relaxed to thermal equilibrium value before a new sequence of pulses begins. In all the experiments undertaken in this work five independent measurements were made and the relaxation data reported in this paper are the average of these individual measurements.

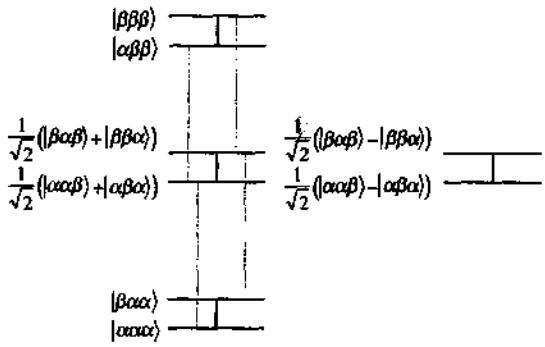

Figure 1. Energy level diagram for a $^{13}CH_2$ spin system. Bold lines indicate allowed carbon transitions while dotted lines stand for allowed proton transitions.

In order to determine seven spectral densities [two dipolar auto-correlation spectral densities (J_{CH}, J_{HH}), two dipolar cross-correlation spectral densities (J_{HCH}, J_{CHH}), and three spin-rotational spectral densities (j_C, j_H, j_{HH})] we have obtained eight experimental data sets for three observable ^{13}C magnetization modes under a variety of different conditions as described below.

^{13}C Inversion Recovery in the Presence of Coupling with Protons. This experiment consists of inverting all three lines of ^{13}C spectrum and monitoring their return to equilibrium in several time delays [pulse sequence: 180° (^{13}C)-t-90°(^{13}C)-AQ]. The results show that the central line relaxes a little faster than any of the two outer lines (see Figure 2(a)). This means that ${}^av_3$ mode can have nonzero magnitude during relaxation which in turn indicates that the cross-correlation spectral density, J_{HCH}, related to ${}^aR_{13}$ can play an important role. From this observation we can also deduce that J_{HCH} is expected to have a negative value.

For the computational purpose the magnetization modes need to be initialized. In the present case the initial and equilibrium conditions are given as

$$ {}^av(0) = K_1 \begin{pmatrix} -1 \\ \sqrt{2}G \\ 0 \\ 0 \end{pmatrix} \quad \text{and} \quad {}^av^T = K_1 \begin{pmatrix} 1 \\ \sqrt{2}G \\ 0 \\ 0 \end{pmatrix}, \qquad (8) $$

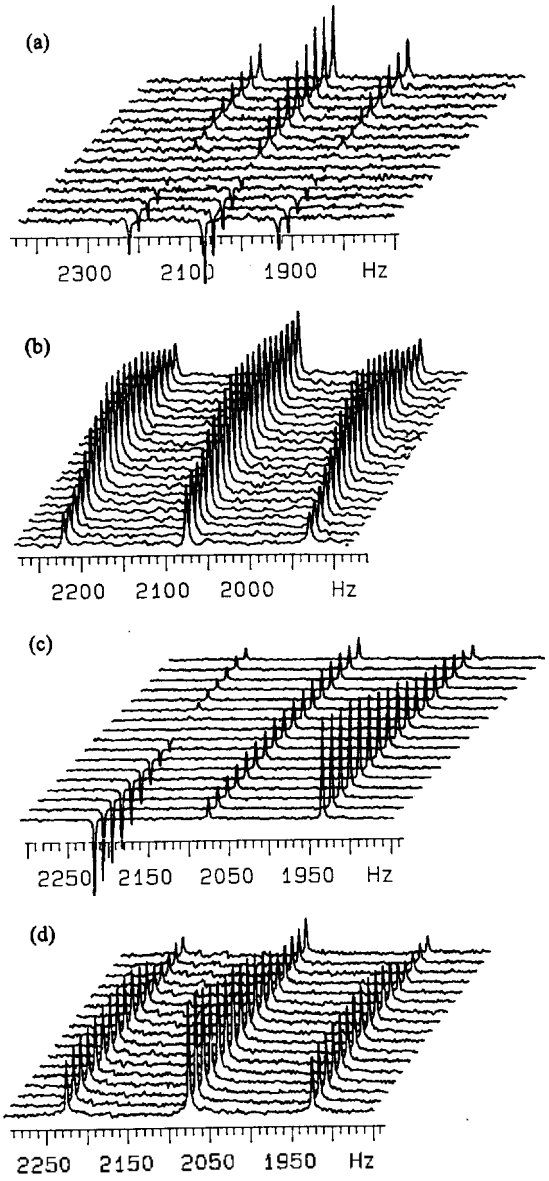

Figure 2. Partially relaxed ^{13}C spectra of various experiment in $CDCl_3$. (a) ^{13}C inversion recovery in the presence of coupling with protons (b) applying a nonselective proton π pulse (c) applying a selective proton π pulse (d) NOE decay in ^{13}C with proton coupled.

where $G=\gamma_H/\gamma_C$. Each of these values has been scaled with respect to the equilibrium intensity of ${}^a v_1$ mode.

From the spectra shown in Figure 3(a) we obtained the T_1 value of *ca* 4.5 sec, and the dipolar spectral density J_{CH} was found to be 0.035 sec^{-1} (initial slope calculation).

Applying a Nonselective Proton π Pulse. This experiment consists of inverting two proton satellite lines simultaneously and monitoring ^{13}C spectrum affected by this perturbation [pulse sequence: 180°(^1H)-t-90°(^{13}C)-AQ]. The initial and equilibrium conditions are

$$ {}^a v(0)=K_2\begin{pmatrix}1\\ -\sqrt{2}\\ 0\\ 0\end{pmatrix} \text{ and } {}^a v^T=K_2\begin{pmatrix}\frac{1}{\sqrt{2}G}\\ 0\\ 0\end{pmatrix} . \quad (9)$$

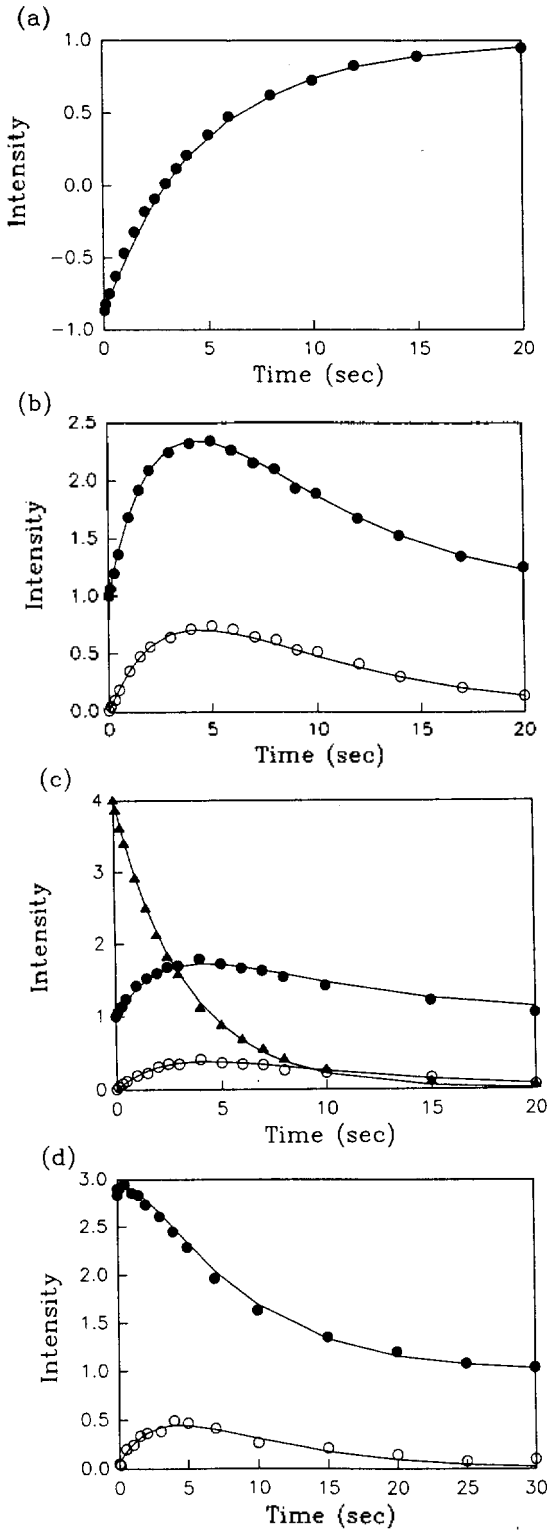

Figure 3. Results of nonlinear regression fit to experimental data in unit of ${}^a v_1^T$ value for $^{13}CH_2$ spin system. (a) ^{13}C inversion recovery in the presence of coupling with protons (b) applying a nonselective proton π pulse (c) applying a selective proton π pulse (d) NOE decay in ^{13}C with proton coupled. Filled circles, empty circles, and filled triangles repesent ${}^a v_1$, ${}^a v_3$, and ${}^s v_1$, respectively.

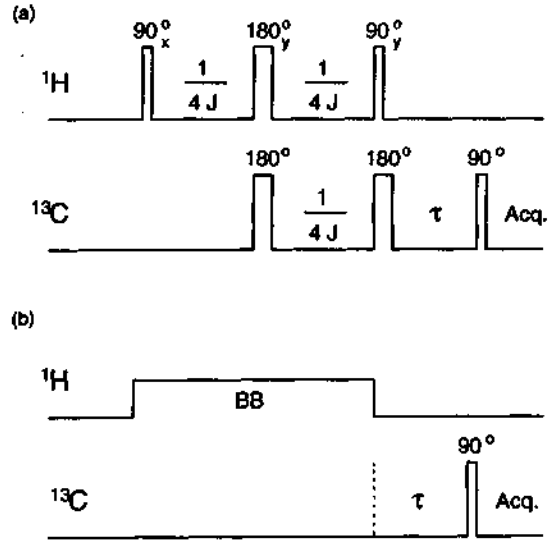

Figure 4. Pulse sequences for (a) selective proton π pulse (b) NOE decay.

From Figure 2(b), which shows the relaxation of ${}^a\nu_1$, and ${}^a\nu_3$ modes, we obtain the information of J_{CH} and J_{CHH}. The outer lines grow faster than the central one with t until they pass through a maximum and begin to shrink. The deviation in the relative intensities from normal 1 : 2 : 1 triplet indicates that the contribution of J_{CHH} to the relaxation affects the outer lines more than the central one. From the initial slopes of ${}^a\nu_1$ and ${}^a\nu_3$ curves [*cf.* Figure 3(b)] we estimated the values of J_{CH} and J_{CHH}, which were found to be about 0.035 and 0.014 sec^{-1}, respectively.

Applying a Selective Proton π Pulse. In this case the symmetric ${}^s\nu_1$ mode can be detected. The observed spectra are shown in Figure 2(c) and the corresponding pulse sequence in Figure 4(a). This pulse sequence inverts only one proton satellite line. By application of such a selective pulse ${}^s\nu_1$ mode is strongly affected but ${}^a\nu_1$ and ${}^a\nu_3$ mode are not as much affected as in the case of applying a nonselective proton π pulse in which both satellite lines are inverted. The initial and equilibrium conditions for this case may be written

$$ {}^a\nu(0) = K_3 \begin{pmatrix} 1 \\ 0 \\ 0 \\ 0 \end{pmatrix}, \qquad {}^a\nu^T = K_3 \begin{pmatrix} 1 \\ \sqrt{2}G \\ 0 \\ 0 \end{pmatrix}, $$

$$ {}^s\nu(0) = K_3 \begin{pmatrix} G \\ 0 \\ 0 \end{pmatrix}, \text{ and } \qquad {}^s\nu^T = K_3 \begin{pmatrix} 0 \\ 0 \\ 0 \end{pmatrix}. \tag{10} $$

From Figure 3(a) we see that the initial ${}^s\nu_1$ value is four times larger than the equilibrium carbon intensity, which can be attributed to the polarization transfer from proton to carbon (as in the case of INEPT experiment). In this case the initial slope calculations show that J_{CHH} is *ca* 0.016 sec^{-1} while J_{CH} is 0.038 sec^{-1}.

NOE Decay in ^{13}C Coupled Spectra. In this experiment, ^{13}C relaxation have been observed without proton decoupling after the full NOE buildup is achieved. The initial and equilibrium conditions in this case are

$$ {}^a\nu(0) = K_4 \begin{pmatrix} 1+\eta \\ 0 \\ 0 \\ 0 \end{pmatrix} \quad \text{and} \quad {}^a\nu^T = K_4 \begin{pmatrix} 1 \\ \sqrt{2}G \\ 0 \\ 0 \end{pmatrix}, \tag{11} $$

where η means the NOE factor.

We obtained η from the initial ${}^a\nu_1$ value which turned out to be very close to its maximum value (≈1.987). We can also evaluate η by making use of spectral densities estimated from the foregone measurements through the following relation:

$$ \eta = \frac{\gamma_H}{2\gamma_C} \frac{J_{CH}(20J_{CH} - 10J_{HCH} + 9j_C) - 10J_{HCH}^2}{(J_{CH} + 3/10J_{HCH})(20J_{CH} - 10J_{HCH} + 9j_C) - 10J_{HCH}^2}, \tag{12} $$

which can be derived from the Solomon equation[24] for a proton decoupled CH_2 spin system.

We can see from Figure 2(d) that the central line relaxes significantly faster than the two outer lines of carbon triplet, which means that the cross-correlation spectral densities, especially J_{CHH}, plays an important role in this spin system.

Calculations

All the calculations made in this work have been carried out numerically since it is not possible to find analytical solutions to the coupled differential equations for AX_2 spin system. We briefly describe the procedure of calculation in what follows. Eq. (7) is more conveniently written in the vectorial form as follows:

$$ \frac{d}{dt} \begin{pmatrix} y_1 \\ y_2 \\ y_3 \\ y_4 \\ \vdots \end{pmatrix} = \begin{pmatrix} R_{11} & R_{12} & R_{13} & R_{14} & \cdots \\ R_{21} & R_{22} & R_{23} & R_{24} & \cdots \\ R_{31} & R_{32} & R_{33} & R_{34} & \cdots \\ R_{41} & R_{42} & R_{43} & R_{44} & \cdots \\ \vdots & \vdots & \vdots & \vdots & \vdots \end{pmatrix} \begin{pmatrix} y_1 \\ y_2 \\ y_3 \\ y_4 \\ \vdots \end{pmatrix} \tag{13} $$

or, more compactly,

$$ \frac{d}{dt} \boldsymbol{y} = \boldsymbol{R}\boldsymbol{y} \tag{14} $$

where $y_i(t) = v_i(t) - v_i^T$. A transformation matrix $\boldsymbol{T}$, which diagonalizes $\boldsymbol{R}$ on similarity transformation, is operated on both side of Eq. (14) to give

$$ \frac{d}{dt} \boldsymbol{Y} = \Lambda \boldsymbol{Y}, \tag{15} $$

where $\boldsymbol{Y} = \boldsymbol{T}\boldsymbol{y}$ and $\Lambda = \boldsymbol{T}\boldsymbol{R}\boldsymbol{T}^{-1}$. Since Λ is assumed to be diagonal, the solutions to Eq. (15), each of which represents a normal mode of magnetization, can be written in the form

$$ y_i(t) = Y_i(0) \exp(\lambda_i t), \tag{16} $$

where λ_i is the ith principal value of the tensor Λ. Now, the original magnetization modes y_i's can be evaluated from Y_i's as

$$ y_i(t) = \sum_j a_{ij} \exp(\lambda_j t) \tag{17} $$

where $a_{ij} = (T^{-1})_{ij} \sum_k T_{jk}\{v_k(0) - v_k^T\}$. Alternatively, Eq. (17) may

Table 2. Spectral densities, dynamic and structural parameters obtained from nonlinear regression fitting

J_{CH} (sec^{-1})	0.0348
J_{HCH} (sec^{-1})	−0.0042
J_{CHH} (sec^{-1})	0.0148
J_{HH} (sec^{-1})	0.0308
j_C (sec^{-1})	0.00004
j_H (sec^{-1})	0.00108
j_{HH} (sec^{-1})	0.00004
∠HCH (degree)	105.1
D_{xx} (sec^{-1})	11.60×10^{10}
D_{yy} (sec^{-1})	1.68×10^{10}
D_{zz} (sec^{-1})	2.38×10^{10}

be rewritten as follows:

$$v_i(t)=v_i^T+\sum_j a_{ij}\ \exp(\lambda_j t) \tag{18}$$

Eight experimental data sets arising from three carbon observable modes ${}^a\nu_1$, ${}^a\nu_3$, and ${}^s\nu_1$ were fitted with Eq. (18) numerically by adjusting seven spectral densities simultaneously until the standard deviation is minimized. Numerical calculations have been performed on IBM PC 486-DX using a least-square fitting program employing the Marquadt algorithm. To facilitate this fitting procedure the approximate values found for some of these spectral densities described in the previous section were taken as the starting values for iterative calculations. The numerical fitting results are shown in Figures. 3(a)-(d) and thus found optimal spectral densities are tabulated in Table 2.

From four dipolar spectral densities obtained in this manner we can extract the information about the geometrical and dynamical properties of the molecule assuming the extreme narrowing condition. For AX_2 system each dipolar spectral density can be expressed as a function of θ(∠HCH) and diffusion tensors as following:[11]

$$J_{ijkl}=\frac{3}{40}\frac{\gamma_i\gamma_j\gamma_k\gamma_l}{r_{ij}^3 r_{kl}^3}\hbar^2\left[\frac{c_1(\theta)}{B_1}+\frac{c_2(\theta)}{B_2}+\frac{c_3(\theta)}{B_3}\right] \tag{19}$$

where γ_i stands for the magnetogyric ratio of ith nucleus and r_{ij} is the internuclear distance between ith and jth nucleus. In the coordinates system shown in Figure 5, where X, Y, and Z denote three principal axes of the diffusion tensor for this system, B_i and $c_i(\theta)$ are defined by

$$\begin{aligned}
B_1&=2D_+ +4D_{zz}\\
B_2&=4D_+ +2D_{zz}+2[(D_{zz}-D_+)^2+3D_-^2]^{1/2}\\
B_3&=4D_+ +2D_{zz}-2[(D_{zz}-D_+)^2+3D_-^2]^{1/2}\\
D_\pm&=\frac{1}{2}(D_{xx}\pm D_{yy})
\end{aligned} \tag{20}$$

and

$$\begin{aligned}
c_1&=12a_{ij}a_{kl}b_{ij}b_{kl}\\
c_2&=d+e\cos\beta+f\sqrt{3}\sin\beta\\
c_3&=d-e\cos\beta-f\sqrt{3}\sin\beta
\end{aligned} \tag{21}$$

where

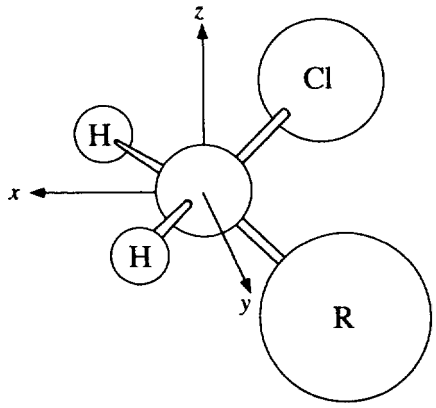

Figure 5. The molecule-fixed coordinates for CH_2 spin system in α,2,6-trichlorotoluene where R represents 2,6-dichlorophenyl group.

$$\begin{aligned}
a_{CH}&=\cos\theta \quad b_{CH}=\sin\theta\\
a_{CH'}&=\cos\theta \quad b_{CH'}=-\sin\theta\\
a_{HH'}&=0 \quad\ \ b_{HH'}=1
\end{aligned} \tag{22}$$

and

$$\begin{aligned}
\beta&=\tan^{-1}(\sqrt{3}D_-/(D_{zz}-D_+))\\
d&=3(a_{ij}^2a_{kl}^2+b_{ij}^2b_{kl}^2)-1\\
e&=1-3(a_{ij}^2b_{kl}^2+a_{kl}^2b_{ij}^2)\\
f&=3b_{ij}^2b_{kl}^2-3a_{ij}^2a_{kl}^2-b_{ij}^2-b_{kl}^2+a_{ij}^2+a_{kl}^2.
\end{aligned} \tag{23}$$

The numerically calculated ∠HCH and diffusion tensors are listed in Table 2.

Conclusions

A great deal of information concerning the relative importance of various relaxation mechanisms can be obtained from the measured spectral densities. From Table 2, we see that the dipolar auto-correlation spectral density, J_{CH}, is much larger than the spin-rotational spectral density, j_C. This means that the relaxation is dominated by the dipolar mechanism rather than the spin-rotational one, which is understandable considering that bulky CH_2Cl group in α,2,6-trichlorotoluene is expected to suffer much more restriction when it undergoes internal rotation than CH_3 group in 2,6-dichlorotoluene. It is also noteworthy that the effect of cross-correlation is comparable to that of auto-correlation. The results obtained in this work show that the effect of cross-correlation can make a significant contribution to the spin-lattice relaxation of AX_2 spin system and can by no means be neglected as has often been assumed. The magnitude of J_{HCH} is found to be significantly smaller than J_{CHH}, which may be attributable to the fact that the three spin orders are seldom generated by a pulse sequence inverting the carbon triplet and that there exist only weak correlation between I_z^C and $I_z^C I_z^H I_z^{H'}$ though the correlation between I_z^H and $I_z^C I_z^H I_z^{H'}$ remains rather strong. We found that the values of spectral densities obtained from the least-square fitting are very close to those estimated from initial slope measurements, which indicates that our initial estimation of some spectral densities was quite

accurate. The calculated NOE factor, η, from dipolar spectral densities and Eq. (11) agrees well with that measured from the spectrum.

From Eq. (19) we calculated the bond angle ∠HCH (105.1°) and the elements of diffusion tensor for CH_2Cl group in the molecule-fixed coordinates shown in Figure 5 by making use of the spectral densities listed in Table 2, assuming that the molecular frame is rigid. The bond angle ∠HCH was found to be somewhat less than the tetrahedral angle 109.5°, which is reasonable considering that the strong repulsions between electrons in the chlorine atom of CH_2Cl and in the dichlorophenyl group can narrow this angle. D_x was found to be several times larger than D_y, and D_z, which means the overall molecular shape and interactions are such that the rotation about the x-axis is more facile than those about the other two axes. The magnitude of these diffusion tensor components also confirms that the extreme narrowing condition is well valid for our case.

Acknowledgment. This research was supported by the SNU-Daewoo Research Fund during the fiscal year of 1993-1994.

References

1. Werbelow, L. G.; Grant, D. M. *J. Chem. Phys.* **1975**, *63*, 544.
2. Mayne, C. L.; Alderman, D. W.; Grant, D. M. *J. Chem. Phys.* **1975**, *63*, 2514.
3. Fuson, M. M.; Prestegard, J. H. *J. Am. Chem. Soc.* **1983**, *105*, 168.
4. Fuson, M. M.; Brown, M. S.; Grant, D. M.; Evance, G. T. *J. Chem. Soc.* **1985**, *107*, 6695.
5. Hu, S. B. *M. S. Thesis*, S. N. U. **1990** "A study of methyl carbon-13 spin-lattice relaxation in 2,6-dichlorotoluene."
6. Wang, C. H.; Grant, D. M. *J. Chem. Phys.* **1976**, *64*, 1522.
7. Mayne, C. L.; Grant, D. M.; Alderman, D. W. *J. Chem. Phys.* **1976**, *65*, 1684.
8. Werbelow, L. G.; Grant, D. M. *Adv. Magn. Reson.* **1977**, *9*, 189.
9. Chenon, M. T.; Bernassau, J. M.; Mayne, C. L.; Grant, D. M. *J. Phys. Chem.* **1982**, *86*, 2733.
10. Fang Liu; Horton, W. J.; Mayne, C. L.; Tian-xiang Xiang; Grant, D. M. *J. Am. Chem. Soc.* **1992**, *114*, 5281.
11. Grant, D. M.; Mayne, C. L.; Fang Liu; Tian-xiang Xiang, *Chem. Rev.* **1991**. *91*, 1591.
12. Vold, R. L.; Vold, R. R.; Canet, D. *J. Chem. Phys.* **1977**, *66*, 1202.
13. Kratchowill, A.; Vold, R. L.; Vold, R. R. *J. Chem. Phys.* **1979**, *71*, 1319.
14. Kratchowill, A.; Vold, R. L. *J. Magn. Reson.* **1980**, *40*, 197.
15. Vold, R. L.; Vold, R. R. *Prog. in NMR Spectrosc.* **1978**, *12*, 76.
16. Canet, D. *Prog. in NMR Spectrosc.* **1989**, *21*, 237.
17. Bain, A. D.; Lynden-Bell, R. M. *Mol. Phys.* **1975**, *33*, 325.
18. Bloch, F. *Phys. Rev.* **1956**, *102*, 104.
19. Wangsness, R. K.; Bloch, F. *Phys. Rev.* **1953**, *89*, 728.
20. Redfield, A. G. *Adv. Magn. Reson.* **1965**, *1*, 1.
21. Bloembergen, N.; Purcell, E. M.; Pound, R. V. *Phys. Rev.* **1948**, *73*, 1679.
22. Pyper, N. C. *Mol. Phys.* **1970**, *19*, 161; **1971**, *21*, 1.
23. Favro, L. D. *Phys. Rev.* **1960**, *119*, 53.
24. Solomon, I. *Phys. Rev.* **1955**, *99*, 559.

A Facile Synthesis of p-Nitrophenyl Glycosides

Shinsook Yoon, DongSung Kim†, and Jeong E. Nam Shin*

Department of Chemistry, Soongsil University, Seoul 156-743, Korea
†Research Lab., Dong-A Pharmaceutical Co. Ltd., Singal Ri, Kyunggi-do 449-900
Received March 2, 1994

Glycosylation of benzoylated glycosyl halides of glucose, galactose and mannose with potassium p-nitrophenoxide and 18-crown-6 complex in chloroform resulted in the stereospecific formation of 1,2-trans p-nitrophenyl glycopyranosides in good yields. The same reaction with benzylated mannopyranosyl chloride gave the α-and β-p-nitrophenyl mannopyranosides in 3 : 1 ratio. However, acetylated 2-azido-altropyranosyl chloride gave β-p-nitrophenyl altropyranoside only.

Introduction

p-Nitrophenyl glycosides are widely used as chromogenic substrates in the study of glycosidase enzymes[1,2], and as linkage arms to couple oligosacchride epitopes to carrier proteins in producing immunogens[2-5]. In the latter, glycosidic p-nitrophenyl groups are converted, *via* an amino function, into a number of groups, such as isothiocyanate, diazo, and N-bromoacetate, capable of reacting with nucleophilic amino acid residues of a protein carrier[1-7]. Such a covalent attachment increases immunogenicity of carbohydrate epitopes. In addition, the coupling may be controlled for the specific synthesis of well-defined antigens, that may enable to elucidate mechanisms of antigen-antibody interaction.

However, conventional methods such as Helferich or Koenig-Knorr reaction have been reported to give p-nitrophenyl